

# Small- $x$ Growth of Nucleon Structure Functions and Its Manifestations in Ultrahigh-Energy Neutrino Astrophysics

A. Z. Gazizov and S. I. Yanush

*B. I. Stepanov Institute of Physics of the National Academy of Sciences of Belarus*

F. Skaryny Ave. 68, 220072 Minsk, Belarus

E-mail: gazizov@dragon.bas-net.by

E-mail: yanush@dragon.bas-net.by

**Abstract.** Rapid growth of neutrino-nucleon cross-sections at high energies due to hypothetical hard pomeron enhancement of  $\nu N$ -structure functions is discussed. Differential and integral hadron moments, which, together with cross-sections, define rates of hadron-electromagnetic cascades in a neutrino detector are calculated for different power-law decreasing neutrino spectra. For comparison two small- $x$  extrapolation schemes are discussed. First includes Regge theory inspired hard pomeron enhancement of  $\nu N$ -structure functions. The second is obtained with the help of trivial extrapolation of perturbative  $QCD$  structure functions from the large  $x$  region to the small  $x$  one. Implications of hard pomeron effects for cross-sections and hadron moments are demonstrated. The most pronounced manifestations are found in integral hadron moments for the case of charged current electron (anti)neutrinos scattering off nucleons.

## 1. Introduction

This paper continues the discussion of some specific features of  $\nu N$  *Deep Inelastic Scattering* (*DIS*) at extremely high, up to  $E_\nu \sim 1 \times 10^{12}$  GeV, energies that was started at the previous Seminar 'NPCS-2000' [1]. The main idea of our approach is to extend the successful small- $x$  description of  $F_2^{ep}(x, Q^2)$  *Structure Function* (*SF*) by A. Donnachie and P. V. Landshoff (*DL*) [2] to  $\nu N$ -*SFs*, namely, to  $F_2^{\nu N}(x, Q^2)$ ,  $F_3^{\nu N}(x, Q^2)$ . *DL* claim that record small- $x$  *ep*-scattering data by *HERA* [3] may be successfully explained with the help of a simple combination of several Regge theory inspired non-perturbative pomerons. The most important are 'soft' pomeron (with intercept  $\sim 1.08$ ) and 'hard' pomeron (with intercept  $\approx 1.4$ ). First prevails at small  $Q^2$ , while the latter dominates at large  $Q^2$ . Moreover, *DL* argue that perturbative  $QCD$  ( $pQCD$ ) fails at small  $x < 10^{-5}$  and that its validity at  $x \sim 10^{-4} \div 10^{-5}$  is a pure fluke. However, one should keep in mind that *DL*'s approach neglects the other, non-leading, poles and cuts in the complex angular momentum  $l$ -plane. This common feature of pomeron physics causes this model to violate the unitarity at  $E_\nu \rightarrow \infty$ .

Using a nontrivial generalization of *DL*'s  $F_2^{ep}(x, Q^2)$  *SF* description to the  $\nu N$ -scattering case, we have constructed  $F_2^{\nu N}(x, Q^2)$  and  $F_3^{\nu N}(x, Q^2)$  *SFs*, presumably valid in the whole range of kinematic variables  $0 \leq x \leq 1$  and  $0 \leq Q^2 \leq \infty$  [1, 4]. At  $x \gtrsim 10^{-5}$  they are chosen to coincide with  $pQCD$  parameterization by *CTEQ5* collaboration [5], while in the small- $x$  region these *SFs* are driven by the analogous Regge theory inspired description. A special interpolation procedure, developed in Ref. [4], allows to meet smoothly these different, both over  $x$  and  $Q^2$  descriptions of *SFs* at low and high  $x$ . In Ref. [1] these *SFs* were denoted

by  $DL+CTEQ5$ , indicating that they have their origin in the interpolation between  $DL$  and  $pQCD$  descriptions.

In parallel there were considered  $SFs$  obtained via simple extrapolation of  $pQCD$   $SFs$  from  $x \geq 1 \times 10^{-5}$  to the small- $x$  region:

$$F_i^{\nu N, Log+CTEQ5}(x < x_{min}, Q^2) = F_i^{\nu N, CTEQ5}(x_{min}, Q^2) \left( \frac{x}{x_{min}} \right)^{\beta_i(Q^2)}, \quad (1)$$

$$\beta_i(Q^2) = \left. \frac{\partial \ln F_i^{\nu N, CTEQ5}(x, Q^2)}{\partial \ln x} \right|_{x=x_{min}}; \quad x_{min} = 1 \times 10^{-5}. \quad (2)$$

These  $SF$ 's smoothly shoot to the low- $x$  region from the  $CTEQ5$  defined high- $x$  one [6, 1, 4]. Starting values of functions and of their logarithm derivatives over  $\ln x$  are taken here at the  $x = x_{min}$  boundary of  $CTEQ5$ . This parameterization was designated as  $Log+CTEQ5$ .

Below we shall evaluate several observables involved in High Energy Neutrino Astrophysics ( $HENA$ ) using both parameterization. We shall compare them so that to reveal the manifestations of hard pomeron enhancement in these values.

## 2. Observables of HENA

An incident cosmic high-energy  $\nu$ -flux can be detected only by registration of secondary particles, the products of  $\nu N$ - and/or  $\nu e$ -collisions with matter (basic ideas of  $HENA$  are expounded in Ref. [7]). Hence, the observables are mostly rates of high-energy muons and/or of nuclear-electromagnetic cascades. In this paper we shall discuss only  $\nu N$ -interactions, though the most remarkable process in  $HENA$  is resonance cascade production via

$$\bar{\nu}_e + e^- \rightarrow W^- \rightarrow \text{hadrons} \quad (1)$$

at  $E_{\bar{\nu}_e} \simeq 6.4 \times 10^{15}$  eV [8, 9]. This resonance should show itself as a narrow high spike in the differential energy spectrum of cascades; at resonance energy it exceeds essentially the ordinary  $\nu N$ -interaction background.

Muons and cascades are produced via  $CC$ -

$$\nu_\mu(\bar{\nu}_\mu) + N \rightarrow \mu^\mp + X \quad (2)$$

and  $NC$ -

$$\nu_\mu(\bar{\nu}_\mu) + N \rightarrow \nu_\mu(\bar{\nu}_\mu) + X \quad (3)$$

$DIS$ . And in special case of electron (anti)neutrino  $CC$ -interaction,

$$\nu_e(\bar{\nu}_e) + N \rightarrow e^\mp + X, \quad (4)$$

both final states contribute to the same cascade, so that the whole energy of an incident neutrino is transferred in it. But the  $NC$ -scattering case of  $\nu_e(\bar{\nu}_e)N$  does not differ from (3).

Differential and integral rates of cascade production in a detector for a model neutrino flux with a power-law decreasing energy spectrum,

$$F_\nu(E_\nu) = A \times E_\nu^{-(\gamma+1)}, \quad (5)$$

where  $\gamma$  is the index of an integral neutrino spectrum  $F_\nu(> E)$  (it is commonly assumed that  $1.1 \leq \gamma \leq 2.1$ ), may be calculated with the help of so-called differential,

$$Z_h(E_h, \gamma) = \int_0^1 dy y^\gamma \frac{d\sigma_{\nu N}(E_h/y, y)}{\sigma_0 dy}, \quad (6)$$

and integral,

$$Y_h(E_h, \gamma) = \gamma \int_0^1 du u^{\gamma-1} Z_h\left(\frac{E_h}{u}, \gamma\right), \quad (7)$$

hadron moments [10, 11]. Here  $E_h$  is the energy of a hadron-electromagnetic cascade,  $y = E_h/E_\nu$  and  $\sigma_0$  is the normalization cross-section; for  $m_W = 81$  GeV  $\sigma_0 = 1.09 \times 10^{-34}$  cm<sup>2</sup>. These rates in  $CC$ -scattering case (2) are

$$dN_h(E_h)/dt = Z_h^{CC}(E_h, \gamma) N_N \sigma_0 \Omega F_\nu(E_h), \quad (8)$$

$$dN_h(> E_h)/dt = Y_h^{CC}(E_h, \gamma) N_N \sigma_0 \Omega F_\nu(> E_h). \quad (9)$$

Here  $N_N$  is the number of nucleons in a detector and  $\Omega$  is an effective solid angle the neutrino flux comes from. The cases of  $\bar{\nu}N$ - and  $NC$ -interactions may be accounted for in a similar way: one is to substitute in (6) the appropriate differential cross-section for the  $CC$  one.

Note that in Eq.s (8,9) both differential and integral neutrino fluxes are taken at the cascade energy  $E_h$  and that for power-law decreasing spectra (5) the following useful relation is valid:

$$\gamma \times F_\nu(> E) = E \times F_\nu(E). \quad (10)$$

In the case of (anti)neutrino  $CC$ -scattering (4) a role of differential hadron moment belongs to the normalized  $CC$ -cross-section,  $\sigma_{\nu N}^{CC}(E_\nu)/\sigma_0$ ; since now  $E_h = E_\nu$ ,  $\nu_e$ -flux in (8,9) is to be taken at the energy of incident neutrino.

### 3. Cross-sections of $\nu N$ -scattering

In parton picture  $\nu N$ -cross-section increases with the energy due to multiplication in number of the nucleon small- $x$  'sea'-quark contents. In the framework of non-perturbative pomeron approach such growth occurs due to specific poles in the complex  $l$ -plane. Calculated within  $DL+CTEQ5$  and  $Log+CTEQ5$  parameterizations,  $CC$  and  $NC$   $\nu(\bar{\nu})N$ -cross-sections are shown in Fig. 1. The most part of high-energy cross-section is accumulated at small  $x$

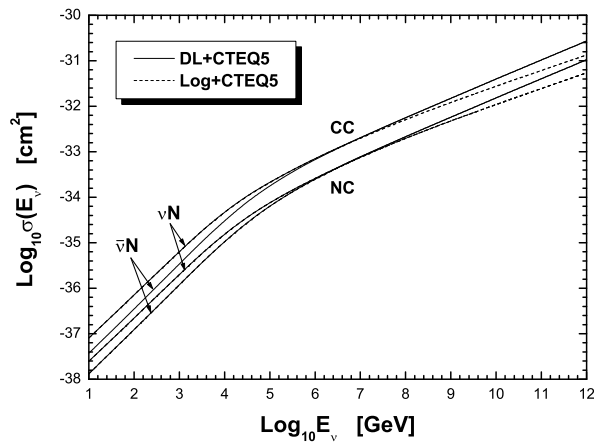


Fig. 1.  $\nu N$  and  $\bar{\nu} N$  cross-sections calculated within  $DL+CTEQ5$  and  $Log+CTEQ5$  models for  $CC$ - and  $NC$ -interactions.

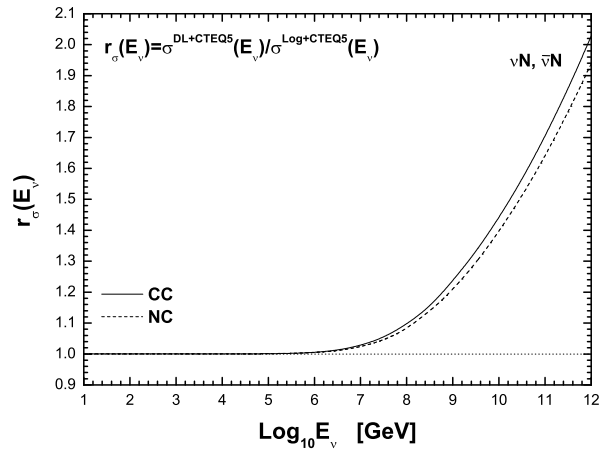


Fig. 2. Ratios of corresponding  $DL+CTEQ5$  and  $Log+CTEQ5$  cross-sections for  $\nu N$ - and (indistinguishable here)  $\bar{\nu} N$ -scattering cases.

and high  $Q^2$  where hard pomeron term dominates  $SFs$ . Since hard pomeron enhanced

$DL+CTEQ5$  small- $x$   $SFs$  are higher than corresponding  $Log+CTEQ5$  ones, their cross-sections prevail over 'perturbative' at high energies. Discrepancies become especially clear in Fig. 2, where ratios of corresponding  $DL+CTEQ5$  and  $Log+CTEQ5$  cross-sections,  $r_\sigma(E_\nu)$ , are plotted versus neutrino energy. The curves for  $\nu N$  and  $\bar{\nu}N$  cases practically coincide in this graph; ratios for  $NC$ -interactions are very close to corresponding  $CC$  ones.

It should be noted, that hard pomeron enhanced growth of  $\nu N$ -cross-sections is the most rapid among all presently known, which have been obtained under different 'ordinary' (no extra dimensions and so on) assumptions (see Ref. [4] and references therein).

#### 4. Differential and integral hadron moments

According to Eq.s (6,7), hadron moments depend on high-energy part of  $\nu$ -spectrum where

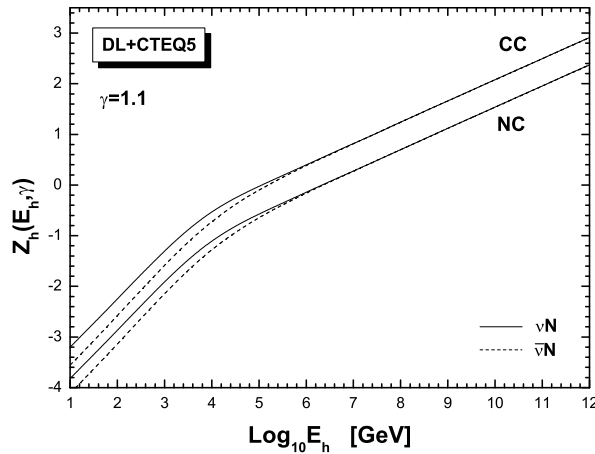


Fig. 3.  $\nu N$  and  $\bar{\nu}N$   $DL+CTEQ5$   $CC$  and  $NC$  differential hadron moments for integral  $\nu$ -spectrum index  $\gamma = 1.1$ .

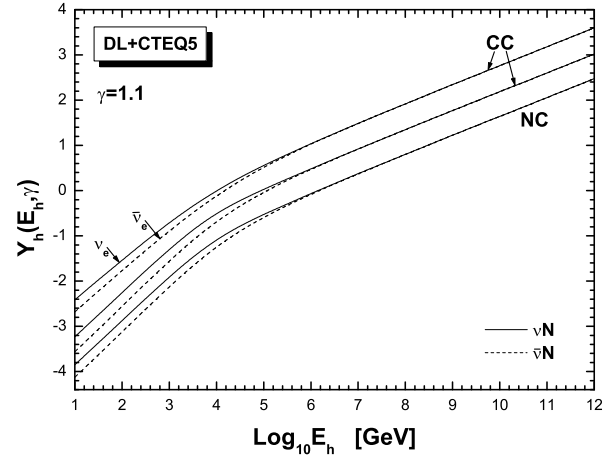


Fig. 4. The same curves as in Fig. 3, but for integral hadron moments.  $\nu_e N$ - and  $\bar{\nu}_e N$ -scattering cases are shown separately.

cross-sections are higher. As a consequence, hard pomeron effects look even more pronounced in these observables. To illustrate a common trend, the differential and integral  $\nu N$  and  $\bar{\nu}N$  hadron moments are plotted in Fig. 3 and Fig. 4, respectively, for  $DL+CTEQ5$  parameterization and  $\gamma = 1.1$ , both for  $CC$ - and  $NC$ -interactions.

Dependencies of  $CC$  and  $NC$  hadron moments on  $\gamma$  are shown in Figs 5,6,7,8 with the help of ratios between corresponding moments with indicated  $\gamma$  and those with  $\gamma = 1.1$ .

And, finally, ratios between corresponding  $CC$  hadron moments of  $DL+CTEQ5$  and  $Log+CTEQ5$  parameterizations are demonstrated in Figs 9,10 for  $\gamma = 1.1$ . Due to sensitivity to higher energies, these ratios are higher than ratios of cross-sections. The most salient difference is seen in  $Y_h^{CC}(E_h, \gamma)$  for  $\nu_e(\bar{\nu}_e)N$  scattering, where the whole energy goes to the cascade.

#### 5. Conclusions

We have demonstrated that small- $x$  hard pomeron enhancement of  $\nu N$  structure functions evinces itself via essential growth of some  $HENA$  observables at high energies. For example, cross-sections and hadron moments, defining rates of cascades, grow more rapidly with the energy than in the case of trivial  $pQCD$  extrapolation. The calculated hadron moments may be used for estimation of cascade rates in future giant high-energy neutrino detectors

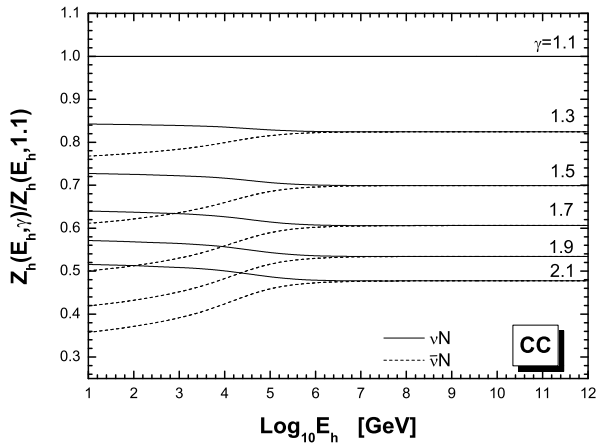


Fig. 5. Ratios for *DL+CTEQ5 CC* differential hadron moments.

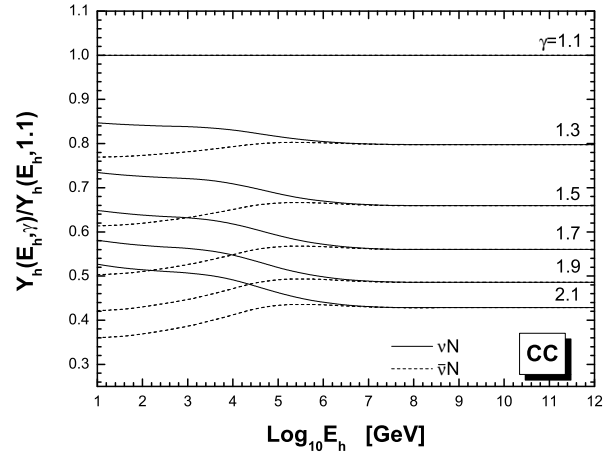


Fig. 6. Ratios for *DL+CTEQ5 CC* integral hadron moments.

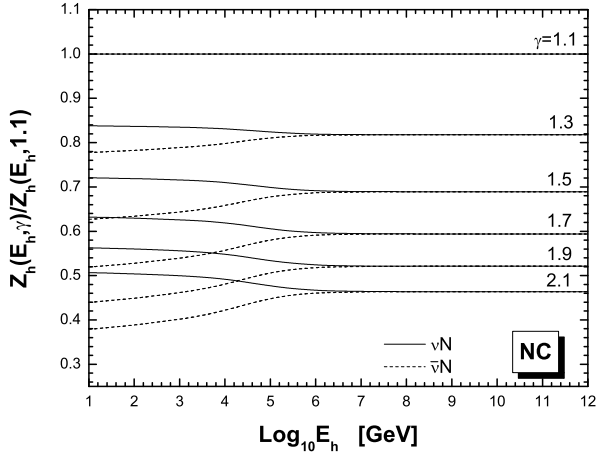


Fig. 7. Ratios for *DL+CTEQ5 NC* differential hadron moments.

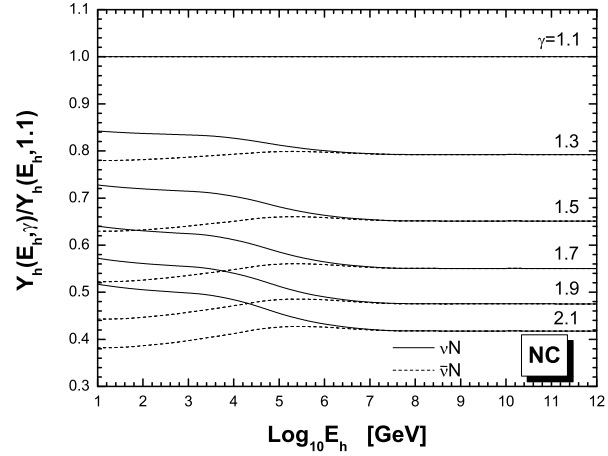


Fig. 8. Ratios for *DL+CTEQ5 NC* integral hadron moments.

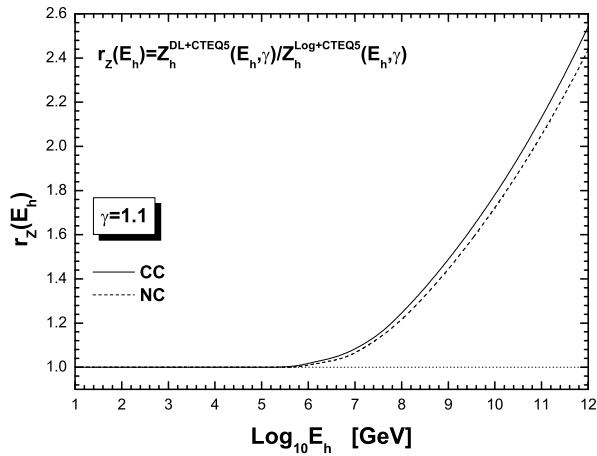


Fig. 9. Ratios between *CC* differential hadron moments of *DL+CTEQ5* and *Log+CTEQ5* parameterizations for  $\gamma = 1.1$ .

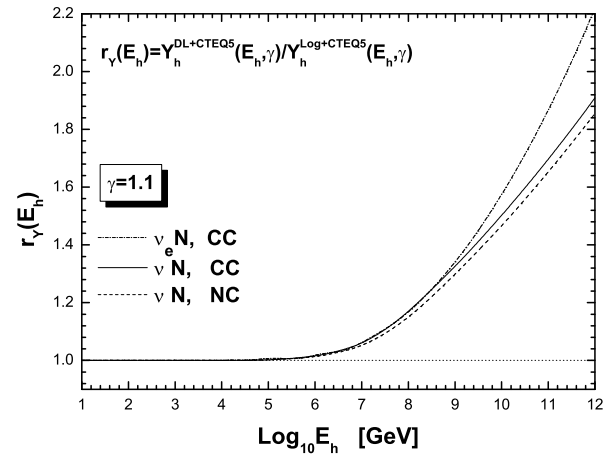


Fig. 10. The same as in Fig. 9, but for integral hadron moments.

## Acknowledgments

## References

- [1] A. Z. Gazizov and S. I. Yanush, in *Proc. of 9th Annual Seminar NPC'S'2000*, edited by L. Babichev and V. Kuvshinov (Institute of Physics, Minsk, 2000), Vol. 9, p. 313.
- [2] A. Donnachie and P. V. Landshoff, Phys. Lett. **437B**, 408 (1998).  
A. Donnachie and P. V. Landshoff, Phys. Lett. **B**, (in press); hep-ph/0105088.
- [3] H1: C. Adloff *et al.*, Nucl. Phys. **B497**, 3 (1997).  
ZEUS: J. Breitweg *et al.*, Phys. Lett. **407B**, 432 (1997).  
H1: C. Adloff *et al.*, Eur. Phys. J. **C21**, 33 (2001).
- [4] A. Z. Gazizov and S. I. Yanush, Phys. Rev. D (2002), (in press); astro-ph/0105368.
- [5] CTEQ collaboration: H. L. La *et al.*, hep-ph/9903282; see also <http://www.phys.psu.edu/~cteq/>.
- [6] V. S. Berezinsky, A. Z. Gazizov, G. T. Zatsepin and I. L. Rozental, Sov. J. Nucl. Phys. **43**, 637 (1986).
- [7] V. S. Berezinsky, S. V. Bulanov, V. A. Dogiel, V. L. Ginzburg and V. S. Ptuskin, *Astrophysics of Cosmic Rays* (North-Holland, Amsterdam, 1990).
- [8] V. S. Berezinsky and A. Z. Gazizov, Sov. Phys. JETP Lett. **25**, 276 (1977).
- [9] V. S. Berezinsky and A. Z. Gazizov, Sov. J. Nucl. Phys. **33**, 230 (1981).
- [10] V. S. Berezinsky and A. Z. Gazizov, Sov. J. Nucl. Phys. **29**, 1589 (1979).
- [11] V. S. Berezinsky and A. Z. Gazizov, in *Proc. of 1979 DUMAND Summer Workshop at Khabarovsk and Lake Baikal* (Hawaii, Honolulu, 1980), p. 202.